Available online at www.sciencedirect.com
ScienceDirect
Biochimica et Biophysica Acta 1757 (2006) 1117–1121
BIOCHIMICA ET BIOPHYSICA ACTA
BBA
www.elsevier.com/locate/bbabio

The K-pathway revisited: A computational study on cytochrome *c* oxidase

Anne Tuukkanen [1], Michael I. Verkhovsky, Liisa Laakkonen, Mårten Wikström*

Helsinki Bioenergetics Group, Institute of Biotechnology, University of Helsinki, FIN-00014 University of Helsinki, Helsinki, Finland

Received 24 March 2006; received in revised form 20 April 2006; accepted 26 May 2006
Available online 7 June 2006

Abstract

Cytochrome *c* oxidase contains two established proton-conducting structures, the D- and K-pathways. The role of the K-pathway appears to be to conduct the first two protons to be used in water formation, which are taken up on reduction of the oxidized enzyme. Previous computational work has suggested that Lys(I)-319 is neutral over a large pH range and in various redox states. We have constructed oxidase models in different redox states using quantum-chemically derived charge parameters for the redox metal centers. The protonation behaviour of titratable sites in the two-subunit enzyme was defined by continuum electrostatics. The calculations reported here show substantial protonation of Lys(I)-319 at neutral pH once the stable X-ray crystallographic water molecule found immediately next to it is treated explicitly. The immediate structure of the Lys(I)-319 environment is independent of redox state, but the pK_a value of this residue changes with the redox state of the binuclear heme a_3/Cu_B site whenever that change is electrically uncompensated. Lys(I)-319 is also found to interact electrostatically with the conserved residue Glu(II)-62 in subunit II. These results are discussed in relation to the role of the K-pathway in oxidase function.
© 2006 Elsevier B.V. All rights reserved.

Keywords: Proton transfer; Electrostatic; Protein structure

1. Introduction

Cytochrome *c* oxidase is a membrane-bound electron transfer protein in the respiratory chain of all eukaryotes and many aerobic bacteria. It catalyses the reduction of dioxygen to water and couples this reaction to pumping of protons across the membrane [1]. Hence, the energy released in O_2 reduction is conserved in the form of an electrochemical proton gradient across the membrane, which may be used, e.g., for the synthesis of ATP (see [2]). The oxidase contains four redox active metal sites (Cu_A, heme *a*, heme a_3 and Cu_B), which form an electron transfer pathway from the electron donor cytochrome *c* to an oxygen molecule bound at the active site (Fig. 1). The electrons are delivered from cytochrome *c* through Cu_A and heme *a* to the binuclear heme a_3/Cu_B center, where the chemistry of oxygen reduction to water takes place [2,3]. Several polar groups and water molecules inside the protein constitute pathways for redox-coupled proton translocation. Protons required for water formation and for pumping are transferred by two different proton-conducting pathways, D and K, named after the highly conserved amino acids (Asp(I)-91 and Lys(I)-319) [2,3].

The protein environment substantially affects the proton affinities (pK_a values) of titratable residues. The low dielectric permittivity of the protein medium modifies pK_a values compared to those measured for titratable groups in aqueous solution. Generally, the membrane environment increases pK_a values of acidic groups and decreases those of basic groups because the neutral forms of amino acid residues are energetically more favoured in the low-dielectric membrane environment. We have calculated the pK_a values of protonatable sites of cytochrome *c* oxidase using continuum electrostatic methods and studied the titration behavior of the key amino acids of the K- and D-pathways and their interaction with the environment. Here, we report new data on the electrostatic properties of Lys(I)-319, the key residue of the K-pathway.

2. Materials and methods

2.1. Structural model

The starting structure for our electrostatic calculations consisted of subunits I and II of the fully oxidized cytochrome *c* oxidase from bovine heart (PDB code

* Corresponding author.
E-mail address: Marten.Wikstrom@helsinki.fi (M. Wikström).
[1] Present address: Institute of Mathematics, Tampere University of Technology, FIN-33101 Tampere, Finland.

0005-2728/$ - see front matter © 2006 Elsevier B.V. All rights reserved.
doi:10.1016/j.bbabio.2006.05.041

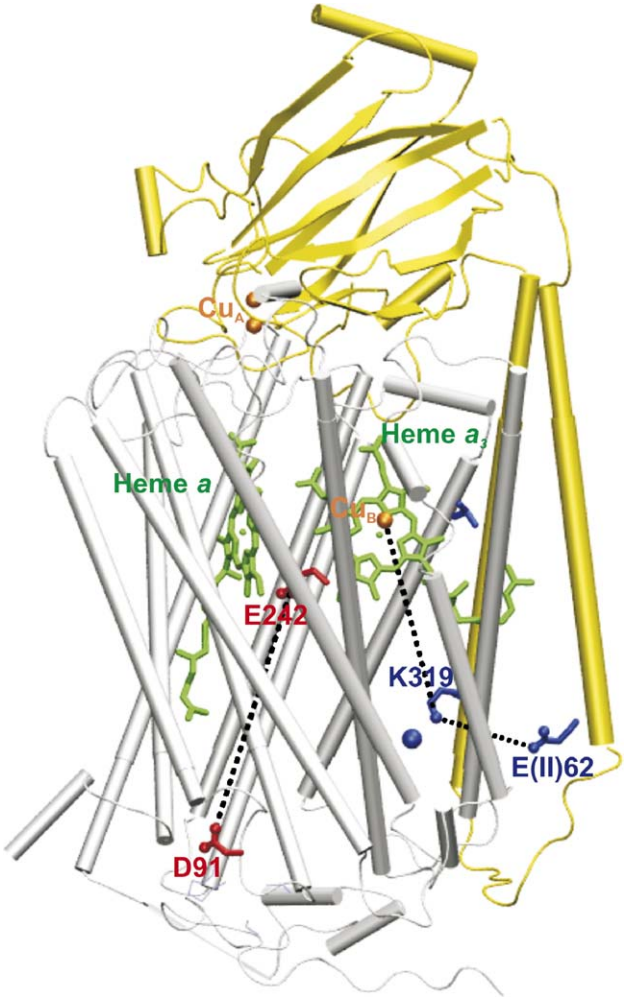

Fig. 1. Structural model of cytochrome *c* oxidase. View of subunits I (grey) and II (yellow) along the membrane plane. Key residues of the D- and K-pathways of proton transfer are indicated along with the four redox-active centers. The blue sphere next to K319 is a crystallographically observed water molecule. Indicated distances between D91 and E242, E(II)62 and K319, and K319 and Cu_B are 24, 9, and 19 Å, respectively. The figure was prepared using the program VMD [26].

1v54, ref. 4), which contain all the redox-active metal centers (Fig. 1). Two heme groups, heme *a* and heme a_3, and a copper atom Cu_B, are located inside the membrane domain of subunit I. Heme *a* is six-coordinated with two axial histidine residues, and Cu_B is ligated by three histidine residues (His(I)-240, His(I)-290 and His(I)-291). The iron-atom of heme a_3 has only one axial histidine ligand. The Cu_A site in subunit II is formed by two copper atoms, which are ligated by two cysteine residues, one histidine residue each, one methionine, and the backbone oxygen of a glutamate residue. The His(I)-290 and His(I)-291 ligands of Cu_B were included as titratable sites in this study, but other metal histidine ligands were not. The coordinates of hydrogen atoms were added using the structure building tool *psfgen* which is part of the program NAMD [7], and the CHARMM27 forcefield [8]. The structure containing subunits I and II, all crystallographic water molecules, and four modeled water molecules in the binuclear center cavity, was relaxed using conjugate gradient energy minimization with NAMD [7] in each studied redox state, before subsequent single-conformer electrostatic calculations.

2.2. Atomic point charges

The CHARMM force field has parameters only for bis-histidine B-type heme, but not for A-type heme or the Cu_B center. Hence, a method to define charges for various intermediates of the cytochrome *c* reaction cycle was needed. The three metal centers in the middle of the protein – heme *a*, heme a_3, and Cu_B – were divided into three separate subsystems. Each subsystem included the metal atom, its immediate ligands, and amino acids or water molecules hydrogen-bonded to the ligands. These three systems were relaxed at the density functional theory (DFT) level, using the hybrid B3LYP functional in connection with a polarized triple-zeta quality basis set (TZVP) for the metals, and a split-valence basis (SVP) for the rest. The torsion angles of the histidines ligating the metals were fixed to their experimental values. Otherwise the surrounding protein environment was modeled as a continuum with a dielectric constant (ε) of 4. After relaxation, a single point without surrounding dielectric ($\varepsilon = 1$) was calculated using TZVP on all atoms. The structure relaxations were performed with Turbomole [9], and the single point CHELPG/RESP calculations with NWChem [10]. The thus obtained RESP charges for the redox-active metal structures were fitted to the existing CHARMM forcefield by scaling the charges on the ligands, so that the net charge equals the sum of the original charges of the force field considered, and by constraining individual atoms on the edges of the calculated QM system to the values in the force field (M.P. Johansson et al., in preparation).

2.3. Electrostatic calculations

The pK_a calculations in this work are based on the assumption that the change in the pK_a value of a titratable site within a protein, compared to the reference pK_a value that the same group has in solution, is only due to electrostatic effects. We used the Multiflex program of the MEAD program package [10] to calculate the electrostatic energies. MEAD describes the protein system semi-macroscopically and uses a finite difference method to solve the Poisson equation numerically. The method employed here divides the energy contributions of the pK_a shift of a titratable site into three parts: the Born solvation energy term (ΔG_{Born}), the background interaction term (ΔG_{back}), and the charge–charge interaction energy between titratable sites (ΔG_{int}). These terms were evaluated with the finite difference method. The sum of the reference pK_a value of the model compound in solution, ΔG_{Born}, and ΔG_{back} terms produces the intrinsic pK_a of a site, which is the pK_a it would have if all other titratable sites were neutral. The final calculated pK_a value of a titratable site depends on its interactions with all other titratable charges and can be obtained using the calculated intrinsic pK_a and knowledge of site–site interaction energies (when the electrostatic energy is known for each configuration). The probability of protonation of a titratable site can be determined by calculating the thermodynamic average over all possible protonation states. However, this is not feasible here since the system includes over one hundred titratable sites and the number of possible protonation states is 2^N, where N is the number of sites. We have therefore used a Metropolis Monte Carlo method to sample a set of low-energy protonation states and to calculate the titration curves of individual titratable sites [11]. The program Karlsberg was used for the Monte Carlo sampling [12,13].

Subunits I and II contain 133 titratable sites; this number includes all titratable amino acid residues (Arg, Asp, His, Lys, Tyr and Glu), the four heme propionates, aquo ligands of heme a_3 and Cu_B, and the His(I)-290 and His(I)-291 ligands of Cu_B. These histidine ligands were found in our calculations to be neutral in the fully oxidized and fully reduced states ([5], but see [6]). We have included a membrane with a thickness of 30 Å as an infinite low dielectric slab in the calculations. The dielectric constant was set to 4 inside the protein medium and in the membrane. Cavities inside the protein were handled as a continuum with a high dielectric constant. Only the water molecules ligating Cu_B, heme a_3, Na^+ and Mg^{2+}, and one stable crystallographic water molecule near Lys(I)-319, were treated explicitly (see below). Otherwise, we used a dielectric constant of 80 in the bulk solution and in the cavities inside the protein. The Poisson equation was solved in three consecutive steps using the grid-focusing method. The first step had a grid resolution of 2.0 Å, the second 0.85 Å, and the final step a resolution of 0.20 Å. The reference pK_a values of titratable sites were: Arg 12.0, Asp 4.0, Glu 4.0, His 6.5, Lys 10.4, Tyr 9.6, heme propionates 4.8. The water ligands of oxidized and reduced Cu_B and heme a_3 were given pK_a values of 9.5 and 15.7, respectively (see [4]).

3. Results

The residue Lys(I)-319 in the K-pathway of proton transfer has been suggested to be neutral over a large pH range and in all tested

redox states on the basis of previous electrostatic calculations [5,6]. The area near Lys(I)-319 is very hydrophobic. However, there is one highly stable water molecule next to the side chain of Lys(I)-319 (Fig. 1), as seen in X-ray crystallographic structures [4], and this water molecule was not explicitly treated in the early calculations. We tested two different approaches: (i) the presumably water-filled cavities inside the enzyme were treated as a continuum with $\varepsilon = 80$ and the aquo ligands of the Cu_B, heme a_3, Na^+ and Mg^{2+} metal centers were modeled explicitly or, (ii) the single water molecule near Lys(I)-319 was also included explicitly. The background interaction energy term, ΔG_{back}, of Lys(I)-319 in the oxidized enzyme increased from 1.8 ΔpK_a units in case (i) to 4.4 ΔpK_a units in case (ii), while the Born solvation energy term, ΔG_{Born}, stayed about the same (−10.9 ΔpK_a). The change in ΔG_{back} is due to interaction of the lysine side-chain with the water molecule. The pK_{half} value of Lys(I)-319 in the oxidized enzyme, the pH value at which it is half-protonated, and the analog of a pK_a value in a multisite system, was found to be 1.4 in case (i) and considerably higher, near neutrality, in case (ii). Henceforth, we will use the latter model.

Glu(II)-62 has been suggested to be an entry point of the K-pathway [14–16, but see 17]. This residue is located in the second transmembrane helix of subunit II, near the N-side surface at an approximately 9 Å distance from Lys(I)-319 (Fig. 1). Early electrostatic calculations suggested that the pK_a value of Glu(II)-62 may be affected by the redox state of the binuclear site [5], and an electrostatic interaction of about 3.6 kcal/mol (2.6 ΔpK_a units) between Lys(I)-319 and Glu(II)-62 was reported. Interestingly, our calculations yielded precisely the same value (*cf.* 14). Fig. 2 shows the titration behaviour of Lys-319 (Fig. 2A) and Glu(II)-62 (Fig. 2B) in the fully oxidized and fully reduced states of the enzyme. Both residues have non-standard titration curves with distinguishable low and high pH transitions, which can be explained by the electrostatic interaction between the two. We have modeled this behavior by a simple scheme that encompasses four states: (A) the fully unprotonated pair, (B) the pair with the lysine protonated, (C) the pair with the glutamate protonated, and (D) the pair with both residues protonated. We define the pK_a for the A/B equilibrium as pK_1, for A/C as pK_2, for B/D as pK_3 and for C/D as pK_4. The electrostatic interaction between the two residues may then be defined as ΔpK, which is equal to both $pK_1 - pK_4$ and $pK_2 - pK_3$. As shown in Fig. 2, the best fit to the lysine titrations yields a fair representation of the results from the electrostatic calculations. The best fit for the oxidized state yielded pK_1 to pK_4 values of 9.20, 9.23, 6.73 and 6.70, and $\Delta pK = 2.50$. The amplitudes of the two transitions in this state were roughly equal in the titration curves of both sites, which is a direct consequence of their similar pK_a values. In the fully reduced enzyme, the equilibrium was shifted towards protonation of Lys(I)-319, and the best fit yielded pK_1 to pK_4 values of 11.20, 10.21, 7.31 and 8.30, and $\Delta pK = 2.9$. This is expected since Lys(I)-319 is closer to the binuclear site. Note that due to the coupling between Lys(I)-319 and Glu(II)-62 the increase in protonation of Lys(I)-319 upon reduction is partially compensated for by deprotonation of Glu (II)-62 in the range pH 7–11 (Fig. 2). It should be noted that the simulation of the electrostatic findings by a simple four-state interaction model is not perfect; deviations are especially clear in the reduced state. This is not unexpected, because the structure includes several other interacting residues, even though such additional interactions are clearly relatively small.

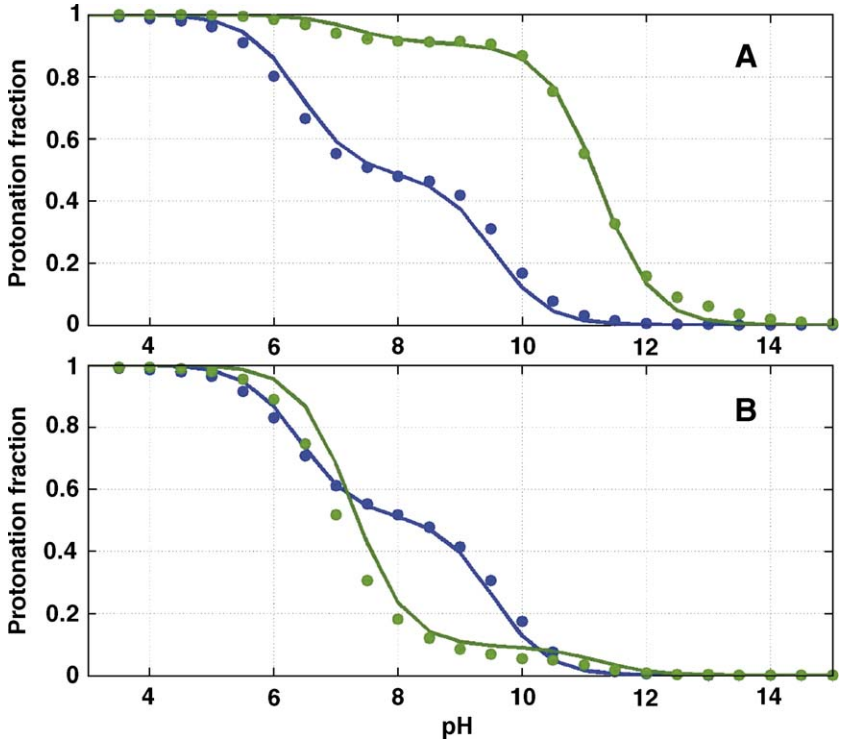

Fig. 2. pH-dependence of the protonated fractions of Lys(I)-319 (A) and Glu(II)-62 (B) in the fully oxidized (blue dots) and fully reduced (green dots) enzyme. The non-standard titration curves have low pH and high pH transitions, which are connected to the 2/1 and 1/0 proton equilibria, respectively, for the lysine/glutamate pair. Solid lines represent the best fit from modeling the interaction (see text).

It is important to emphasize that in the structural model tested here, the fully oxidized binuclear center had an OH^- ligand on ferric heme a_3, an aquo ligand on cupric Cu_B, and a protonated Tyr(I)-244. The electrostatic calculations showed that full reduction of this site is coupled to protonation of the heme a_3 ligand to water, and since no other charge compensation occurred, reduction increased the net charge of the center by −1 unit. In contrast, reduction of heme a_3 alone, which was also coupled to protonation of its OH^- ligand, did not affect the overall charge of the center. Interestingly, in this latter case no significant change in the pK_a values of Lys(I)-319 or Glu(II)-62 were found (not shown; see below).

4. Discussion

Electrostatic calculations using quantum-chemically defined partial charges of the redox centers show that Lys(I)-319 is substantially protonated in the oxidized enzyme at pH 7. The difference with respect to previous calculations [5,6] is mainly due to explicit treatment of a water molecule near Lys(I)-319, rather than assigning $\varepsilon = 80$ for the cavity around this residue. The same effect of the water molecule, although with different numerical values, was obtained in our initial calculations with ad hoc charges. However, our quantum-chemically derived charges should represent the electronic structure in a more realistic way. Structured water molecules can have significant effects on the stability of ionized states of titratable sites inside a protein. However, calculations without treating water molecules explicitly often agree better with experiments because the exact orientation of water molecules is not known from the crystallographic structure, and because water molecules might be highly mobile, which can make their modeling as static permanent dipoles unrealistic [18]. Here, the high stability of the hydrogen bond between Lys(I)-319 and the nearby water molecule during the minimization procedures in different redox states indicates the importance of this specific interaction, and justifies explicit modeling of this water molecule. In addition, we found that the intrinsic pK_a of Lys(I)-319 is raised considerably on reduction of the binuclear site (and less so for Glu (II)-62), but only provided that such reduction is not charge-compensated. We also found a strong electrostatic interaction between Lys(I)-319 and Glu(II)-62 (cf. 5,14), which has the effect of splitting the "titration" of both residues into two transitions over a relatively wide pH range. We emphasize that the exact protonation state of the oxidized binuclear center is not known, and that different forms of this state (state O) have been discussed [19,20]. However, we believe that our major result may nevertheless be generalized. The high occupancy of the protonated form of Lys(I)-319 upon uncompensated electron transfer to the binuclear site makes the possibility quite attractive that the K-pathway functions as a "dielectric well", as proposed by Rich et al. [21]. Indeed, Brändén et al. [22] predicted that the water molecule found near Lys(I)-319 might affect its pK_a, as we report here, and suggested that the protonated side-chain of Lys(I)-319 might in such a case swing towards the binuclear center to partially compensate for the charge of the electron. Such electron transfer, not associated with net proton uptake, occurs in the $A \rightarrow P_R$ transition of the catalytic cycle, where an electron from heme a moves into the binuclear site and the O − O bond of O_2 is broken [23,24]. We recently showed that this reaction is linked to internal transfer of a proton across approximately one third of the dielectric. Most of this could be ascribed to proton transfer from Glu(I)-242 to a site above the heme groups, because the effect was almost completely abolished by mutating the Glu to Gln [25]. However, a very small fraction of vectorial proton transfer remained in this mutant, which we ascribed to local proton transfer from Tyr(I)-240 to the oxygen ligand of heme a_3. The data presented here suggest that this remaining effect might include increased protonation of Lys(I)-319.

Our results are consistent with the proposals than the conserved Glu(II)-62 residue is of functional importance [14–16,21,22]. Glu (II)-62 may be an entrance point of the K-pathway, but another significant function may be the modulating effect on the titration behavior of Lys(I)-319, as found here. Finally, we stress that the proposed dielectric buffering function of the K-pathway [21,22] does not exclude a role for this pathway also in net proton transfer from the N-side of the membrane to the binuclear site during reduction of that site. From available data it appears that dielectric buffering by the K-pathway may be required during the "oxidative" phase of the catalytic cycle, whereas net proton transfer may be required during the "reductive" phase. It is still enigmatic, however, how proton transfer via this path to the binuclear site is shut down during the "oxidative" phase.

5. Conclusions

We have shown here that Lys(I)-319, the name residue of the K-pathway of proton transfer, is significantly protonated at neutral pH, in contrast to what has been generally believed. Moreover, the pK_a of this residue is raised significantly upon electrically uncompensated reduction of the binuclear center. Due to electrostatic interactions, neither Lys(I)-319 nor Glu(II)-62 titrate in the conventional Henderson–Hasselbalch fashion, but the extent of protonation of each shows pH-dependence over a wide pH range. These findings require reconsideration of the function of the K-pathway.

Acknowledgements

Financial support was obtained from the Sigrid Jusélius Foundation, Biocentrum Helsinki and the Academy of Finland. We acknowledge Mikael P. Johansson for providing the RESP charges of the metal sites, and the Finnish National Center of Scientific Computing (CSC) for computing resources.

References

[1] M.K.F. Wikström, Proton pump coupled to cytochrome *c* oxidase in mitochondria, Nature 266 (1977) 271–273.
[2] R.B. Gennis, Coupled proton and electron transfer reactions in cytochrome oxidase, Front. Biosci. 9 (2004) 581–591.
[3] P. Brzezinski, Redox-driven membrane-bound proton pumps, TIBS 29 (2004) 380–387.
[4] T. Tsukihara, K. Shimokata, Y. Katayama, H. Shimada, K. Muramoto, H. Aoyama, M. Mochizuki, K. Shinzawa-Itoh, E. Yamashita, M. Yao, Y. Ishimura, S. Yoshikawa, The low-spin heme of cytochrome *c*

oxidase as the driving element of the proton-pumping process, Proc. Natl. Acad. Sci. U. S. A. 100 (2003) 15304–15309.
[5] A. Kannt, C.R.D. Lancaster, H. Michel, The coupling of electron transfer and proton translocation: electrostatic calculations on *Paracoccus denitrificans* cytochrome c oxidase, Biophys. J. 74 (1998) 708–721.
[6] D.M. Popović, A.A. Stuchebrukhov, Electrostatic study of the proton pumping mechanism in bovine heart cytochrome c oxidase, J. Am. Chem. Soc. 126 (2004) 1858–1871.
[7] J.C. Phillips, R. Braun, W. Wang, J. Gumbart, E. Tajkhorshid, E. Villa, C. Chipot, R.D. Skeel, L. Kale, K. Schulten, Scalable molecular dynamics with NAMD, J. Comput. Chem. 26 (2005) 1781–1802.
[8] A.D. MacKerell Jr., et al., All-atom empirical potential for molecular modeling and dynamics studies of proteins, J. Phys. Chem., B 102 (1998) 3586–3616.
[9] R. Ahlrichs, M. Bär, M. Häser, H. Horn, C. Kölmel, Electronic structure calculations on workstation computers: the program system turbomole, Chem. Phys. Lett. 162 (1989) 165–169.
[10] E. Aprà, et al., NWChem, A Computational Chemistry Package for Parallel Computers, Version 4.6, Pacific Northwest National Laboratory, Richland, Washington 99352-0999, USA, 2004.
[11] D. Bashford, K. Gerwert, Electrostatic calculations of the pK_a values of ionizable groups in bacteriorhodopsin, J. Mol. Biol. 224 (1992) 448–473.
[12] P. Beroza, D.R. Fredkin, M.Y. Okamura, G. Feher, Protonation of interacting residues in a protein by a Monte Carlo method: application to lysozyme and the photosynthetic reaction center, Proc. Natl. Acad. Sci. U. S. A. 88 (1991) 5804–5808.
[13] B. Rabenstein (1999). Karlsberg online manual. http://lie.chemie.fu-berlin/karlsberg/.
[14] J. Ma, P.H. Tsatsos, D. Zaslavsky, B. Barquera, J.W. Thomas, A. Katsonouri, A. Puustinen, M. Wikström, P. Brzezinski, J.O. Alben, R.B. Gennis, Glutamate-89 in subunit II of cytochrome bo3 from *Escherichia coli* is required for the function of the heme-copper oxidase, Biochemistry 38 (1999) 15150–15156.
[15] M. Brändén, F. Tomson, R.B. Gennis, P. Brzezinski, The entry point of the K-proton-transfer pathway in cytochrome c oxidase, Biochemistry 41 (2002) 10794–10798.
[16] F.L. Tomson, J.E. Morgan, G. Gu, B. Barquera, T.V. Vygodina, R.B. Gennis, Substitutions for glutamate 101 in subunit II of cytochrome c oxidase from *Rhodobacter sphaeroides* result in blocking the proton-conducting k-channel, Biochemistry 42 (2003) 1711–1717.
[17] O.-M.H. Richter, K.L. Dürr, A. Kannt, B. Ludwig, F.M. Scandurra, A. Giuffrè, P. Sarti, P. Hellwig, Probing the access of protons to the K pathway in the *Paracoccus denitrificans* cytochrome *c* oxidase, FEBS J. 272 (2005) 404–412.
[18] C.J. Gibas, S. Subramaniam, Explicit solvent models in protein pK_a calculations, Biophys. J. 71 (1996) 138–147.
[19] M.I. Verkhovsky, A. Jasaitis, M.L. Verkhovskaya, J.E. Morgan, M. Wikström, Proton translocation by cytochrome *c* oxidase, Nature 400 (1999) 480–483.
[20] D. Bloch, I. Belevich, A. Jasaitis, C. Ribacka, A. Puustinen, M.I. Verkhovsky, M. Wikström, The catalytic cycle of cytochrome *c* oxidase is not the sum of its two halves, Proc. Natl. Acad. Sci. U. S. A. 101 (2004) 529–533.
[21] S. Jünemann, B. Meunier, R.B. Gennis, P.R. Rich, Effects of mutation of the conserved lysine-362 in cytochrome *c* oxidase from *Rhodobacter sphaeroides*, Biochemistry 36 (1997) 14456–14464.
[22] M. Brändén, H. Sigurdson, A. Namslauer, R.B. Gennis, P. Ädelroth, P. Brzezinski, On the role of the K-proton transfer pathway in cytochrome *c* oxidase, Proc. Natl. Acad. Sci. U. S. A. 98 (2001) 5013–5018.
[23] P. Ädelroth, M. Ek, P. Brzezinski, Factors determining electron transfer rates in cytochrome *c* oxidase: investigation of the oxygen reaction in the *R. sphaeroides* and bovine enzymes, Biochim. Biophys. Acta 1367 (1998) 107–117.
[24] S. Paula, A. Sucheta, I. Szundi, Ó. Einarsdóttir, Proton and electron transfer during the reduction of molecular oxygen by fully reduced cytochrome *c* oxidase: a flow-flash investigation using optical multichannel detection, Biochemistry 38 (1999) 3025–3033.
[25] I. Belevich, M.I. Verkhovsky, M. Wikström, Proton-coupled electron transfer drives the proton pump of cytochrome *c* oxidase, Nature 440 (2006) 829–832.
[26] W. Humphrey, A. Dalke, K. Schulten, VMD: visual molecular dynamics, J. Mol. Graph. 14 (1996) 33–38.